

Mammalian cryptochromes impinge on cell cycle progression in a circadian clock-independent manner

Eugin Destici,^{1,2} Małgorzata Oklejewicz,¹ Shoko Saito^{1,3} and Gijsbertus T.J. van der Horst^{1,*}

¹Department of Genetics; Center for Biomedical Genetics; Erasmus University Medical Center; Rotterdam, The Netherlands; ²Department of Medicine; School of Medicine; University of California, San Diego; San Diego, CA USA; ³Graduate School of Comprehensive Human Sciences; Institute of Basic Medical Sciences; University of Tsukuba; Tsukuba, Japan

Key words: circadian clock, cryptochromes, cell cycle, DNA damage response, transcriptome analysis

Abbreviations: SCN, suprachiasmatic nuclei; MDF, mouse dermal fibroblast; MEF, mouse embryonic fibroblast; WT, wild type; CCG, clock-controlled gene; DDR, DNA damage response; IR, ionizing radiation; qRT-PCR, quantitative reverse transcription-polymerase chain reaction

By gating cell cycle progression to specific times of the day, the intracellular circadian clock is thought to reduce the exposure of replicating cells to potentially hazardous environmental and endogenous genotoxic compounds. Although core clock gene defects that eradicate circadian rhythmicity can cause an altered in vivo genotoxic stress response and aberrant proliferation rate, it remains to be determined to what extent these cell cycle related phenotypes are due to a cell-autonomous lack of circadian oscillations. We investigated the DNA damage sensitivity and proliferative capacity of cultured primary *Cry1*^{-/-}/*Cry2*^{-/-} fibroblasts. Contrasting previous in vivo studies, we show that the absence of CRY proteins does not affect the cell-autonomous DNA damage response upon exposure of primary cells in vitro to genotoxic agents, but causes cells to proliferate faster. By comparing primary wild-type, *Cry1*^{-/-}/*Cry2*^{-/-}, *Cry1*^{+/-}/*Cry2*^{-/-} and *Cry1*^{-/-}/*Cry2*^{+/-} fibroblasts, we provide evidence that CRY proteins influence cell cycle progression in a cell-autonomous, but circadian clock-independent manner and that the accelerated cell cycle progression of *Cry*-deficient cells is caused by global dysregulation of *Bmal1*-dependent gene expression. These results suggest that the inconsistency between in vivo and in vitro observations might be attributed to systemic circadian control rather than a direct cell-autonomous control.

Introduction

Oscillatory systems are recurring phenomena in biology. Some well-studied examples are the circadian clock, generating daily rhythms in behavior, physiology and metabolism,¹ and the cell cycle, driving the periodic duplication of the genome and subsequent cell division.²

Circadian clocks are present in most organisms and have a periodicity of about (ca.) one day (dies). In mammals, the central clock is located in the suprachiasmatic nucleus (SCN) of the hypothalamus. The SCN transmits information to peripheral organs by releasing humoral factors (e.g., peptides, hormones) that synchronize cell-autonomous clocks in peripheral tissues.^{1,3} Remarkably, even cultured cells display circadian rhythms that are asynchronous in a population, but can be synchronised by various compounds that impinge on different pathways (e.g., cAMP and glucocorticoid signaling).^{4,5} The circadian system orchestrates various physiological processes, e.g., sleep-wake cycle, metabolism, blood pressure, hormone secretion, cell cycle division and DNA repair.^{1,6,7} In the human population and in

animal models, chronic desynchrony with the light-dark cycle (e.g., chronic jetlag or frequent shift work) and genetic disruption of circadian rhythmicity have been linked to various pathologies such as cancer, obesity, cardiovascular disease and mental disorders.⁸⁻¹¹

At the molecular level, the circadian clock consists of a cell autonomous oscillator, composed of a set of clock genes and proteins that act in interlocked transcription/translation feedback loops. The only essential loop for circadian rhythmicity is a negative feedback loop in which the CLOCK/BMAL1 transcriptional activator drives expression of the *Cryptochrome* (*Cry1* and *Cry2*) and *Period* (*Per1* and *Per2*) genes via E-box promoter elements. After a delay, the CRY and PER proteins accumulate in the cytoplasm, heterodimerize, and subsequently enter the nucleus, where they shut down expression of their own genes by inhibiting CLOCK/BMAL1-mediated transcription.¹²⁻¹⁴ In addition, auxiliary feedback loops such as cyclic expression of the *Bmal1* gene, confer robustness and precision to the core negative feedback loop.^{15,16} The CLOCK/BMAL1 and PER/CRY complexes also underlie cyclic expression of a series of E-box

*Correspondence to: Gijsbertus T. J. van der Horst; Email: g.vanderhorst@erasmusmc.nl
Submitted: 07/05/11; Revised: 08/24/11; Accepted: 09/06/11
<http://dx.doi.org/10.4161/cc.10.21.17974>

containing clock-controlled genes (CCGs), that connect the circadian oscillator to rhythmic output processes. These CCGs vary from tissue to tissue, probably reflecting the specific requirements of each tissue.^{17,18} Among the CCGs are transcription activators and inhibitors, circadian expression of which indirectly drives cyclic expression of other genes. Transcription profiling studies have shown that the circadian clock allows up to 10% of a tissue's transcriptome to oscillate.^{19–22}

Among these genes are many genes involved in the cell cycle, which may allow the circadian clock to gate cell cycle progression to defined moments of the day. In fact, the evolutionary advantage for an organism to replicate its genome when the risk of DNA damage induction (e.g., through solar UV-radiation or metabolically produced oxidative stress) is lowest, has been postulated to constitute the driving factor for the naissance of the circadian clock.²³ It has been shown for a variety of mammalian tissues (e.g., human and rodent skin and intestinal tract; mouse bone marrow) that cells preferably divide at a defined time of the day, implying circadian gating of cell cycle progression.^{24–26} Likewise immortalized mouse embryonic fibroblasts (NIH 3T3) have been reported to preferentially divide at three distinct circadian time points,²⁷ although such correlation between circadian clock phase and cell division was not observed in another immortalized rodent cell line (Rat-1).²⁸

Recent studies with mutant and knockout mouse models for core clock genes revealed various cell cycle-related phenotypes, ranging from increased ionizing radiation-induced carcinogenesis to enhanced genotoxic stress sensitivity and an impaired DNA damage Response (DDR).^{29–35} Moreover, most of the core clock genes (especially *Per1* and *Per2*) display altered expression levels in tumors, while oppositely, enforced modulation of clock gene expression can affect the proliferation rate and apoptosis sensitivity of cancer cells.³⁶ Surprisingly, recent studies have shown that the connection between the clock and the DDR is reciprocal: activation of the DDR by genotoxic exposure leads to phase shifting of the circadian clock in *Neurospora*, mammalian cells, as well as free-running mice.^{37–39} While the full implications of the latter observations have not yet been elucidated, they are further indications strengthening the intertwinement of the circadian clock and cell cycle related processes.

Despite recent progress, several fundamental questions with respect to the coupling of the circadian clock and the cell cycle remain largely unanswered. For instance, it is not clear whether the observed cell cycle alterations in circadian clock mutant cells or tumor cells with altered clock gene expression levels are due to alterations in the molecular oscillator itself or due to clock-independent functions of core clock proteins. Furthermore, as peripheral clock output processes are not only controlled by a local circadian clock,^{17,18} but also (in)directly by the SCN central clock via cyclically released hormones, peptides or other compounds (including growth factors) that may affect peripheral clock output pathways,⁴⁰ it remains to be resolved whether the circadian clock controls cell cycle progression cell-autonomously or systemically.

In the present study, we investigated the DNA damage sensitivity and proliferative capacity of cultured primary fibroblasts

from various circadian clock mutant mouse models. Our results show that the circadian clock does not control the cell cycle and DDR at the cell-autonomous level, but rather suggest a systemic mechanism for in vivo circadian control of the cell cycle and DDR.

Results

Normal genotoxic stress response in circadian clock-deficient *Cry1^{-/-}|Cry2^{-/-}* cells. To investigate the impact of the circadian clock on the DDR, we isolated isogenic (C57BL/6J) primary mouse embryonic fibroblasts (MEFs) from wild-type (WT) and circadian clock-deficient *Cry1^{-/-}|Cry2^{-/-}* embryos, as well as primary dermal fibroblasts (MDFs) from the skin of adult mice⁴¹ and maintained the cells at low oxygen (3%) to reduce oxidative stress and delay onset of replicative senescence.⁴² Next, cells were exposed to various genotoxic stress conditions. A comparison of the cellular survival of WT and *Cry1^{-/-}|Cry2^{-/-}* MDFs upon exposure to increasing doses of UV light reveals normal UV sensitivity of the mutant cells (Fig. 1A). Likewise, the sensitivity of *Cry1^{-/-}|Cry2^{-/-}* MEFs to chronic oxidative stress (induced by transferring culture dishes to 20% oxygen) or ionizing radiation (IR), determined by measuring the relative proliferation capacity of cells following treatment, is in the WT range (Figs. 1B and C).

Next, we investigated the response of *Cry1^{-/-}|Cry2^{-/-}* MEFs upon exposure to IR (4 Gy) in more detail. Using expression of the key p53-target gene *p21* (encoded by *Cdkn1a*) as a read-out, we show that p53 activation in *Cry1^{-/-}|Cry2^{-/-}* MEFs, is in the WT range (Fig. 1D). Likewise, FACS analysis of the cell cycle distribution of IR exposed *Cry1^{-/-}|Cry2^{-/-}* MEFs revealed a depletion of S-phase cells and an accumulation of G₁-phase cells, comparable to that observed in WT cells (Fig. 1E). Together, these results suggest that DNA damage/p53-mediated cell cycle arrest is normal in primary *Cry1^{-/-}|Cry2^{-/-}* cells.

Collectively, these data show that under in vitro conditions, genotoxic stress sensitivity, DDR and cell cycle check points are not perturbed in clock-deficient *Cry1^{-/-}|Cry2^{-/-}* fibroblasts.

Accelerated cell cycle progression of circadian clock-deficient *Cry1^{-/-}|Cry2^{-/-}* cells. Interestingly, while we did not observe any difference in their ability to respond to genotoxic stress, primary *Cry1^{-/-}|Cry2^{-/-}* MEFs displayed a higher proliferation rate than primary WT MEFs under unstressed low oxygen culture conditions (Fig. 2A), although not as profoundly as, for example, the very rapidly growing *p53^{-/-}* MEFs⁴³ (see also Fig. S2A). This difference was consistently observed using WT and *Cry1^{-/-}|Cry2^{-/-}* MEF lines (n = 3–4; obtained from different litters) and was independent of cell passage number (Fig. 2B). Similar results were obtained using primary mouse dermal fibroblasts (MDFs) from adult WT and *Cry1^{-/-}|Cry2^{-/-}* mice and an alternative cell proliferation assay method (Fig. S1). To proliferate faster, cells must shorten one or more phases of the cell cycle (mainly G₁ or G₂). We therefore compared the cell cycle distribution of proliferating cultures of WT, *Cry1^{-/-}|Cry2^{-/-}* and *p53^{-/-}* MEFs by FACS analysis. In line with their reported shorter G₁ phase,⁴⁴ *p53^{-/-}* cell cultures contain a reduced percentage of cells in G₁ phase (Fig. 2C). In contrast, *Cry1^{-/-}|Cry2^{-/-}* MEFs showed a phase distribution that strongly

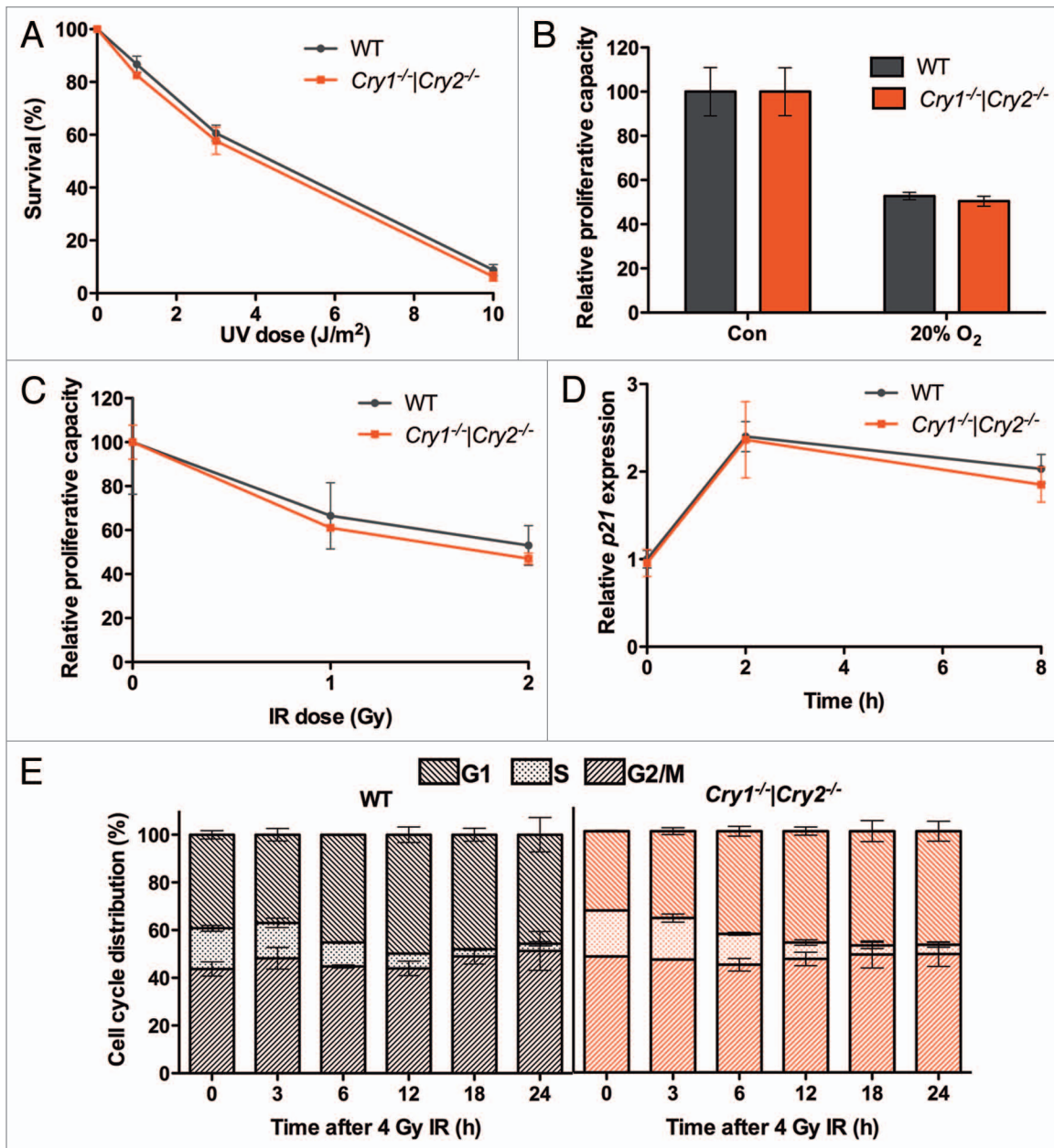


Figure 1. Normal response of primary *Cry*-deficient fibroblasts to genotoxic stress. (A) UV sensitivity of primary WT and *Cry1^{-/-}|Cry2^{-/-}* MEFs (n = 3 independent cell lines per genotype). Survival was determined by ³H-Thymidine incorporation 3 d after exposure of cells to increasing doses of UV-B light (254 nm). (B) Oxidative stress sensitivity of WT and *Cry1^{-/-}|Cry2^{-/-}* MEFs (n = 4 independent cell lines per genotype), as determined by measuring the relative proliferative capacity under 3% and 20% oxygen. Cells were counted 3 d after start of the treatment. (C) Ionizing radiation (IR) sensitivity of WT and *Cry1^{-/-}|Cry2^{-/-}* MEFs (n = 2 independent cell lines per genotype), as determined by measuring the relative proliferative capacity of cells after exposure to 1 or 2 Gy of IR. (D) G₁ checkpoint activation in IR-exposed primary WT (n = 4) and *Cry1^{-/-}|Cry2^{-/-}* MEFs (n = 3). Activation of p53 was determined by RT-PCR analysis of *p21* gene expression 2 and 8 h after exposure of cells to 4 Gy of IR. Two replicate samples per individual cell line were analyzed. Gene expression was normalized against *Hprt* expression and the *p21* expression level at t = 0 was set as 1. (E) Cell cycle arrest of IR exposed primary WT and *Cry1^{-/-}|Cry2^{-/-}* MEFs (n = 3 per genotype) as determined by FACS analysis. Each treated cell line was normalized to its own mock-treated control (set to 100%) for the sensitivity studies. Error bars indicate the standard error of the mean (SEM).

resembled that of WT cells (Fig. 2C). The normal G₁/G₂ phase distribution in *Cry1^{-/-}|Cry2^{-/-}* MEFs suggests that both cell cycle phases are equally shortened in the absence of CRY proteins.

Accelerated cell cycle progression in *Cry1^{-/-}|Cry2^{-/-}* cells is clock-independent. The faster cell cycle progression of *Cry1^{-/-}|Cry2^{-/-}* MEFs might originate from either the inactivation of the

circadian core oscillator or the specific absence of CRY proteins (and accordingly a clock-associated or a yet unknown clock-independent function of these proteins). To distinguish between these two possibilities, we made use of the observation that *Cry1^{-/-}|Cry2^{-/-}* mice maintain (long period) rhythmicity in constant darkness, while *Cry1^{-/-}|Cry2^{-/-}* mice become arrhythmic after

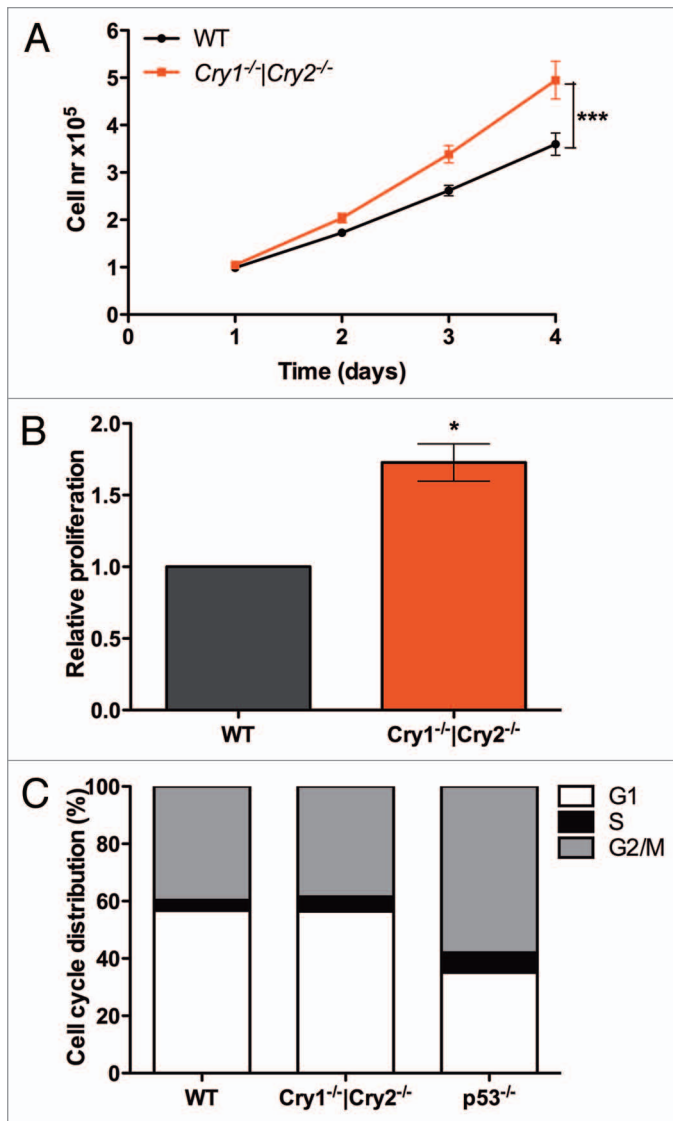


Figure 2. Accelerated cell cycle progression of primary *Cry*-deficient MEFs. (A) Proliferation curves of WT ($n = 4$) and *Cry1*^{-/-}|*Cry2*^{-/-} ($n = 3$) primary MEF lines. Cells (1×10^5 /well) were seeded in triplicate in 6-well plates on day 0 and counted on subsequent days. Curves were compared after fitting an exponential growth curve ($***p < 0.001$). (B) Quantification of the relative proliferation rate of WT and *Cry1*^{-/-}|*Cry2*^{-/-} MEFs from four experiments using cell lines from different litters and/or different passage. To correct for inter-experimental variability, within each experiment the proliferation rate of the WT cells was set to 1 and the proliferation rate of the *Cry1*^{-/-}|*Cry2*^{-/-} cells is expressed relative to that ($*p < 0.05$; column statistics). (C) Cell cycle phase distribution analysis of WT, *Cry1*^{-/-}|*Cry2*^{-/-} cells and *p53*^{-/-} MEFs. Cells were collected and fixed one day after seeding and cell cycle distribution was determined by FACS analysis. Error bars indicate the SEM.

several days.⁴¹ We isolated primary MEFs from *Cry1*^{+/-}|*Cry2*^{+/-} and *Cry1*^{-/-}|*Cry2*^{+/-} embryos and transduced the cells with a lentiviral *Per2::luciferase* reporter construct to allow real time imaging of circadian clock performance in vitro. In line with recent observations, suggesting that cellular circadian phenotypes can be more extreme as compared with mouse behavior or oscillations in the SCN,^{45,46} we observed that, like *Cry1*^{-/-} and *Cry2*^{-/-} cells,

respectively,⁴⁶ *Cry1*^{-/-}|*Cry2*^{+/-} MEFs show severely impaired/absent oscillations, while *Cry1*^{+/-}|*Cry2*^{-/-} MEFs oscillate robustly (Fig. 3A).

We next compared the proliferation rate of the various *Cry*-deficient MEF lines and observed that *Cry1*^{-/-}|*Cry2*^{+/-} cells and *Cry1*^{+/-}|*Cry2*^{-/-} cells both proliferate faster ($p < 0.001$) than WT MEFs (Fig. 3B). Moreover, the proliferation rate of *Cry1*^{+/-}|*Cry2*^{-/-} cells was significantly lower than that of *Cry1*^{-/-}|*Cry2*^{-/-} cells ($p < 0.01$), while the proliferation rate of *Cry1*^{-/-}|*Cry2*^{+/-} cells showed a similar trend ($p = 0.075$). This finding suggests that the increased proliferation rate of *Cry1*^{-/-}|*Cry2*^{-/-} MEFs cannot be attributed to the absence of a circadian clock in those cells. Rather, as one active copy of the *Cry* genes (either *Cry1* or *Cry2*) is sufficient to partially attenuate the accelerated growth associated with *Cry1*^{-/-}|*Cry2*^{-/-} MEFs, our results suggest that the *Cry* gene products impinge on proliferation capacity in a dose-dependent manner, regardless of whether cells are clock-proficient or clock-deficient.

Neither *Cry* genes nor the circadian clock function as a barrier against hyperproliferation. In view of the previous findings, the question arises whether (circadian clock-proficient) primary cells with a known hyperproliferation phenotype (such as *p53*^{-/-} MEFs, see Fig. S2A) display reduced expression of the *Cry* genes. Bioluminescent imaging of *p53*^{-/-} dermal fibroblasts infected with a lentiviral *Per2::luciferase* reporter construct reveals robust circadian oscillations under confluent conditions (Fig. S2B). Having shown that *p53* deficiency does not affect the circadian clock, we next examined the *Cry1* and *Cry2* mRNA levels in proliferating primary *p53*^{-/-} and WT MEFs by quantitative reverse transcription-PCR (qRT-PCR) analysis. As we used non-clock synchronized cells, the detected expression levels of oscillating genes represent the average expression level. As shown in Figure S2C, *p53*-deficient MEFs show *Cry1* and *Cry2* mRNA levels that are indistinguishable from WT MEFs. Along with our finding that *p53*^{-/-} cells maintain circadian rhythmicity, this suggests that neither reduced expression of *Cry* genes nor clock disruption is a prerequisite for accelerated cell cycle progression.

Accelerated cell cycle progression in *Cry1*^{-/-}|*Cry2*^{-/-} cells is BMAL1-dependent. The CRY proteins are potent inhibitors of CLOCK/BMAL1-induced transcription activation of core clock and clock-controlled E-box genes.^{12,13} Accordingly, the accelerated proliferation rate of *Cry1*^{-/-}|*Cry2*^{-/-} MEFs might originate from constitutive high expression of CLOCK/BMAL1-target genes. We therefore asked the question whether inactivation of *Bmal1* (causing constitutive low expression of CLOCK/BMAL1-target genes and arrhythmicity⁴⁷) would slow down proliferation of *Cry1*^{-/-}|*Cry2*^{-/-} MEFs. To this end, we isolated primary WT and *Bmal1*^{-/-} MEFs, as well as *Bmal1*^{+/-}|*Cry1*^{-/-}|*Cry2*^{-/-} and *Bmal1*^{-/-}|*Cry1*^{-/-}|*Cry2*^{-/-} MEFs and determined their proliferation rate. Two independent experiments with one cell line indicate that an additional *Bmal1* deficiency reduces the proliferation rate of *Cry1*^{-/-}|*Cry2*^{-/-} cells (Fig. 3A). *Bmal1* deletion alone, causing constitutively low expression of CLOCK/BMAL1-target genes, does not appear to alter the proliferation rate of MEFs (Fig. 3B). From these data we conclude that the clock-independent accelerated cell cycle progression phenotype of *Cry1*^{-/-}|*Cry2*^{-/-} cells requires, at

least in part, the presence of *Bmal1*, and may thus originate from constitutive high expression of CLOCK/BMAL1-target genes.

Transcriptome analysis of proliferating WT and *Cry1^{-/-}|Cry2^{-/-}* MEFs. In view of the observed BMAL1-dependency of the accelerated proliferation of *Cry1^{-/-}|Cry2^{-/-}* cells, and given the finding that various cell cycle-related genes oscillate *in vivo* and are in part affected by the *Clock* gene,³³ we first determined by qRT-PCR whether core clock and cell cycle genes are differentially expressed in proliferating *Cry1^{-/-}|Cry2^{-/-}* cells. As shown in Figure 4A, the CLOCK/BMAL1 targets *Per2* and *Dbp* are significantly upregulated in proliferating *Cry1^{-/-}|Cry2^{-/-}* MEFs, while *Bmal1* is downregulated, which is in full agreement with the available data for non-proliferating *Cry*-deficient cells and tissues.⁴⁸⁻⁵⁰ For clarity, we wish to mention here that in the absence of CRY-mediated negative feedback, the low expression level of *Bmal1* is still sufficient to allow intermediate to high expression of CLOCK/BMAL1-driven E-box containing clock(-controlled) genes.⁴⁹ This includes *Rev-erb α* , upregulation of which in *Cry1^{-/-}|Cry2^{-/-}* MEFs leads to downregulation of *Bmal1*¹⁵ and other ROR-driven genes.³⁴ In addition, we measured the expression of a few clock-controlled cell cycle genes (Fig. 4A). Except for *Wee1*,³⁰ none of the other genes tested appeared differentially expressed (Fig. 5A), i.e., *c-Myc*, which has been found to be upregulated in *Per2*-deficient livers,²⁹ and *p21* and *Pten*, which were downregulated in *Cry1^{-/-}|Cry2^{-/-}* livers (unpublished data). Yet, as the WEE1 kinase is an inhibitor of G₂/M transition (by keeping CDK1/cyclin B inactive during the S and G₂ phase), upregulation of *Wee1* is unlikely to explain the hyperproliferative phenotype of the *Cry*-deficient MEFs.

To gain a comprehensive view of gene expression alterations in proliferating *Cry1^{-/-}|Cry2^{-/-}* MEFs (as compared with WT MEFs), we performed an Affymetrix full mouse genome microarray study. We found ~3,000 out of ~45,000 probe sets to display significantly changed expression levels between WT and proliferating *Cry1^{-/-}|Cry2^{-/-}* MEFs ($p \leq 0.05$ and a ≥ 1.2 -fold change up or downregulated). For the genes initially analyzed by qRT-PCR, the array data well fit the PCR findings (Fig. 4A), except for *p21*, for which the transcriptome study indicated a slight downregulation in *Cry1^{-/-}|Cry2^{-/-}* cells. The top 200 up- and downregulated probe sets in *Cry1^{-/-}|Cry2^{-/-}* MEFs are listed in Table S1. Among the upregulated genes are several cyclins and cyclin-dependent kinases (CDKs), while some CDK-inhibitors are downregulated (Table S2), which is consistent with the hyperproliferative phenotype of these cells. Ingenuity Pathway analysis of the entire data set (significant 2,846 probe sets) revealed that various cell cycle-related processes were among the top dysregulated processes (Fig. 4B and Table S1). The three most significant process maps are graphically represented in Figures S4–6. Most of the genes that belong to these pathways show only mild expression changes (~1.5 to 2-fold, Table S1), suggesting that altered expression of a larger group of genes is most likely responsible for the increased proliferation in *Cry*-deficient MEFs.

Discussion

Over the last decade, it has become evident that both cell cycle progression and the DNA damage response (DDR) are linked to

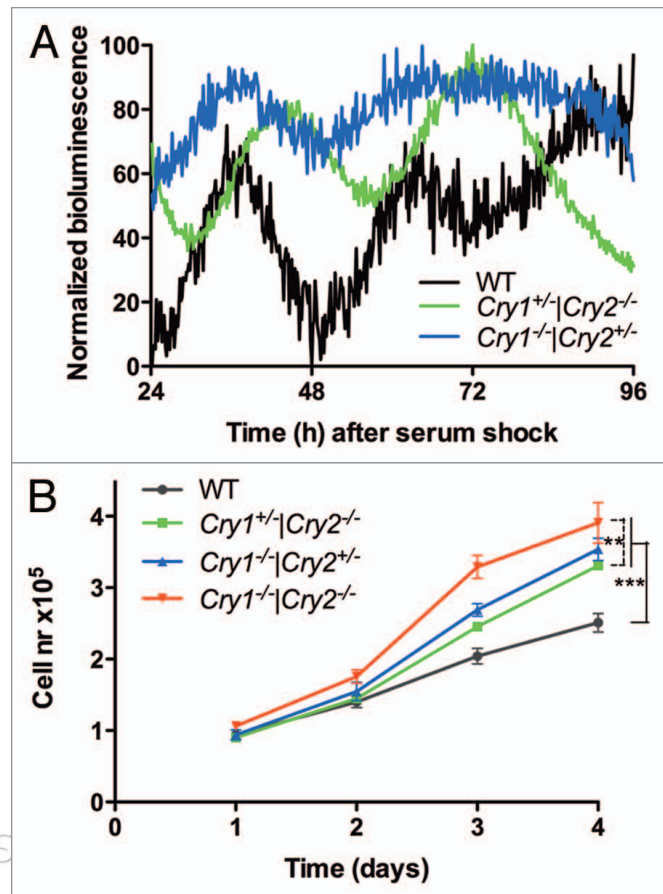


Figure 3. Circadian oscillations do not impede proliferation. (A) Analysis of the circadian clock in *Cry1^{+/-}|Cry2^{-/-}* and *Cry1^{-/-}|Cry2^{+/-}* cells transduced with lentiviral *Per2::luciferase*. Confluent cell cultures were clock-synchronized by serum shock. Raw data was normalized by setting the lowest value to 0 and the highest to 100. (B) Proliferation rate of WT and mutant MEFs ($n = 3$ independent cell lines per genotype). Cells were analyzed as before. Error bars indicate the SEM. Curves were compared by fitting an exponential growth curve (** $p < 0.01$, *** $p < 0.001$).

the circadian system. The circadian clock is thought to gate cell division and to restrict DNA replication to a defined moment of the day and has been shown to influence the adverse effects of genotoxic compounds (chronotoxicity).⁸ These notions stem mainly from *in vivo* observations and accordingly do not discriminate between a cell-autonomous and/or systemic contribution of the circadian clock to these processes. In the present study, we have used primary, arrhythmic *Cry1^{-/-}|Cry2^{-/-}* MEFs, cultured at low (and accordingly more physiological) oxygen concentration to test whether and how the cell-autonomous clock contributes to the cell cycle and DDR.

The circadian clock and the DNA damage response. When exposing primary *Cry1^{-/-}|Cry2^{-/-}* cells to several genotoxic challenges (i.e., UV light, IR, increased oxygen), *Cry1^{-/-}|Cry2^{-/-}* cells turned out to respond in a similar manner as wild-type cells, showing that absence of circadian rhythms and complete loss of *Cry* expression do not impede the DDR. These findings are consistent with a previous report from the Sancar lab addressing the genotoxic sensitivity of *Cry*-deficient cells, although the cells

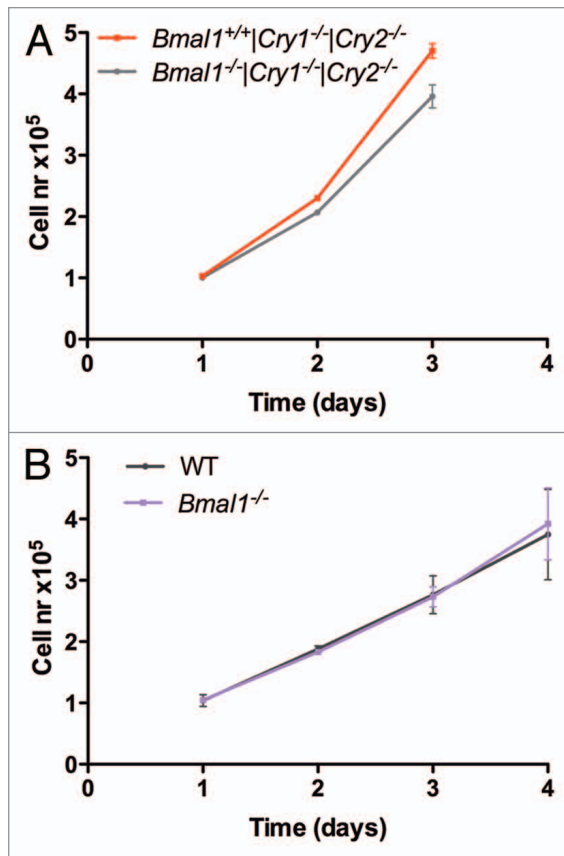


Figure 4. Gene expression analysis of proliferating primary Cry-deficient MEFs. (A) qRT-PCR and microarray analysis of selected clock and cell cycle-related genes in proliferating primary *Cry1*^{-/-}|*Cry2*^{-/-} MEF lines (n = 3 for qPCR, n = 4 for microarrays), as compared with (non-clock synchronized) proliferating WT MEF lines (n = 4 for both techniques). Note that different cell lines were used for qRT-PCR and microarray analysis. The dashed line indicates the WT level (set to 1). *p < 0.05, **p < 0.01, ***p < 0.001; Student t-test. (B) List of top 5 over-represented molecular and cellular functions. Transcriptome analysis was performed on proliferating primary WT and *Cry1*^{-/-}|*Cry2*^{-/-} MEF (4 independent cell lines per genotype). The Ingenuity Pathway Analysis tool was used on differentially expressed genes (p < 0.05) with a ± 1.2-fold change. The p value range (Fisher exact test) indicates the significance range of the various pathways and processes belonging to that function.

used in that study were spontaneously immortalized cells.⁵¹ Yet, as shown in the same study, the absence of circadian rhythms and/or *Cry* genes can affect the DDR, but only in the context of an additional p53 deficiency.³⁵ The normal genotoxic stress sensitivity of primary *Cry1*^{-/-}|*Cry2*^{-/-} MEFs markedly contrasts an in vivo study in which *Cry1*^{-/-}|*Cry2*^{-/-} mice were shown to be less sensitive to the genotoxic agent cyclophosphamide, possibly due to increased resistance of B-cells in the bone marrow, representing the main target organ of this carcinogen.³² Although we currently cannot exclude that this discrepancy results from cell type-specific differences, a more attractive hypothesis would be that the circadian clock in vivo controls the DDR through a systemic mechanism. In support of this view is the recent observation that p53 activity, a major determinant of the DDR, oscillates in vivo through a non-cell-autonomous mechanism that involves

central clock controlled signals from the sympathetic nervous system.⁵²

The circadian clock and cell cycle progression. Interestingly, we observed that primary *Cry1*^{-/-}|*Cry2*^{-/-} MEFs proliferate faster than their wild-type counterparts. Given the normal cell cycle phase distribution of proliferating *Cry1*^{-/-}|*Cry2*^{-/-} MEFs, accelerated growth likely involves shortening of both the G₁- and G₂-phase. This finding contrasts a previous report in which dermal fibroblasts from *Cry1*^{-/-}|*Cry2*^{-/-} mice were shown to proliferate at the same rate as WT cells.⁵¹ This discrepancy may well originate from the fact that this study was performed with spontaneously immortalized cells, grown at atmospheric (20%) oxygen tension (keeping the cell under chronic oxidative stress), whereas we used primary cells cultured at physiological (3%) oxygen levels.

How do our findings relate to other in vitro studies with circadian clock mutant or knockout models addressing cell cycle related phenotypes? Like the *Cry1*^{-/-}|*Cry2*^{-/-} fibroblasts, *Per1/2*-deficient mouse osteoblasts proliferate faster in a cell-autonomous manner.³¹ In contrast, primary *Clock* mutant MEFs and primary *Bmal1*^{-/-} mouse hepatocytes were both shown to proliferate at a reduced rate.^{33,34} Taking into consideration that CLOCK and BMAL1 activate transcription of E-box genes whereas, oppositely, CRY proteins inhibit CLOCK/BMAL1-mediated transcription, the converse phenotype of *Cry1*^{-/-}|*Cry2*^{-/-} cells (i.e., accelerated proliferation) would be in good agreement with this observation. Yet, in the present study primary *Bmal1*^{-/-} MEFs fail to show a reduced proliferation rate, which again may be attributed to differences in cell type i.e., fibroblasts vs. hepatocytes or culture conditions (i.e., low vs. high oxygen tension). On the other hand, the data obtained with *Bmal1*^{-/-} hepatocytes, can also be explained by assuming that it is not the proliferation rate that is altered, but rather the cell cycle re-entry of the hepatocytes, which until the moment of isolation may have been in a quiescent state in the mouse liver. Consistent with this interpretation, the reported decreased proliferation rate of *Clock* mutant MEFs is only observed under conditions where cells in a quiescent state are induced to re-enter the cell cycle.³³

At first sight, the increased proliferation rate of *Cry1*^{-/-}|*Cry2*^{-/-} cells seems consistent with the hypothesis that the circadian clock gates cell cycle progression. This gating would be absent in the arrhythmic *Cry1*^{-/-}|*Cry2*^{-/-} cells. However, the accelerated proliferation rate of *Cry1*^{-/-}|*Cry2*^{-/-} cells does not seem to originate from the inactivation of the circadian clock in these cells. Rather it appears determined by the level of *Cry* gene expression, as clock-proficient (*Cry1*^{-/-}|*Cry2*^{-/-}) and clock-impaired (*Cry1*^{-/-}|*Cry2*^{+/-}) MEFs, both carrying one active *Cry* allele, proliferate faster than WT cells, though not as fast as the double knockout cells. The immediate consequence of our finding that it is not the absence of circadian oscillations, and by inference circadian gating, that is causing the increase in proliferation. Although our results do not exclude cell cycle gating in WT cells, a very recent report provides evidence against a correlation between cell cycle division and circadian phase in cultured immortalized rat fibroblasts expressing a luciferase reporter for the cell cycle or the circadian clock.²⁸

Although our results suggest that the increased proliferation of *Cry1^{-/-}|Cry2^{-/-}* cells is independent of an intact circadian clock, by deleting *Bmal1* (which encodes the only known transcription factor to be inhibited by the CRY proteins), in a *Cry1^{-/-}|Cry2^{-/-}* background, we found that the hyperproliferative phenotype *Cry1^{-/-}|Cry2^{-/-}* cells is at least in part dependent on the presence of *Bmal1*. In the absence of a reduced proliferation rate of *Bmal1^{-/-}* MEFs (as compared with WT MEFs), and given the increased proliferation rate of clock-proficient *Cry1^{+/-}|Cry2^{-/-}* and clock-deficient *Cry1^{-/-}|Cry2^{+/-}* MEFs, we propose that it is the constitutively higher expression of CLOCK/BMAL1-target genes that is driving the increased proliferation in *Cry1^{-/-}|Cry2^{-/-}* MEFs regardless of whether these genes oscillate or not. Since it seems that gene expression changes in circadian genes are less profound in asynchronous, cultured MEFs than they are in vivo (e.g., in the liver), it seems likely that it is the concerted action of a larger number of genes, each with a small change in expression, that underlie the alteration in proliferation in the *Cry1^{-/-}|Cry2^{-/-}* MEFs. Consistent with this, we found widespread differential expression of cell cycle related pathways in the *Cry1^{-/-}|Cry2^{-/-}* MEFs. Another interesting aspect to emerge from our microarray study is the dysregulation of various inflammatory and chemokine signaling genes in *Cry1^{-/-}|Cry2^{-/-}* MEFs. These pathways have recently been linked to oncogene-induced senescence⁵³ and may thus shed some light on how BMAL1 plays a role in (p53-dependent) oncogene-induced senescence in human fibroblasts, as suggested by results from an RNAi screen.⁵⁴

The circadian clock and cell cycle gating: cell autonomous vs. systemic cues? Seminal experiments from the Okamura lab revealed that liver regeneration after partial hepatectomy is gated by the circadian clock and that this gating is absent in *Cry1^{-/-}|Cry2^{-/-}* mice.³⁰ Furthermore, they found that the proliferation of *Cry1^{-/-}|Cry2^{-/-}* hepatocytes was slower.³⁰ As elegant as these experiments are, they do not distinguish between systemic and cell-autonomous control. Based on our results and those of others,⁵² we propose that, as also suggested by our data on the control of the circadian central clock over the DDR, that in vivo gating of the cell cycle occurs through a systemic mechanism. In this context it is interesting to note that several studies demonstrate that liver regeneration is affected by systemic signals,⁵⁵ some of which (e.g., TNF α and IL-6) are known to be secreted in a circadian manner.⁵⁶ Thus, our hypothesis that the circadian system controls cell cycle through systemic cues, could also explain why hepatocytes of *Cry*-deficient mice proliferate slower after partial hepatectomy in vivo³⁰ instead of proliferating faster like the primary *Cry*-deficient fibroblasts in vitro, as we demonstrate here.

In conclusion, our results provide a new view on how the circadian system is connected to the cell cycle and DDR and provide interesting avenues for further investigation.

Methods

Mice. *Cry1*- and *Cry2*-knockout mice have been described before in reference 47, and were backcrossed > 7 times with C57BL/6J mice. *Bmal1*-knockout mice in a C57BL/6J background were generated in the Bradfield lab⁴⁷ and provided by Prof. Franck

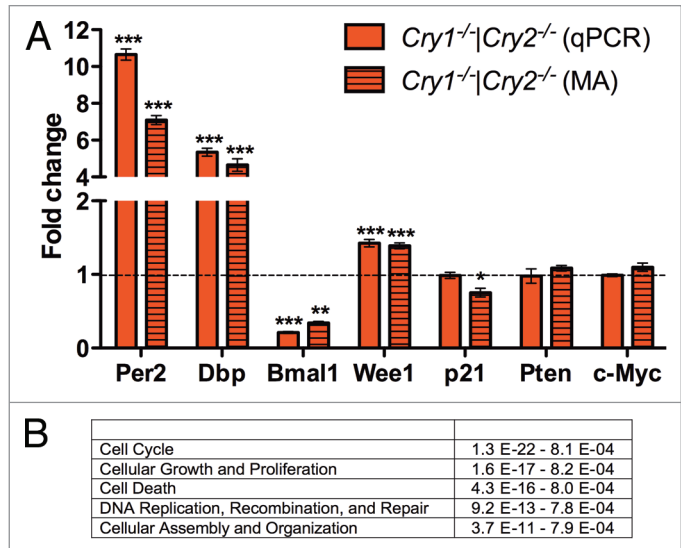


Figure 5. Gene expression analysis of proliferating primary *Cry*-deficient MEFs. (A) qRT-PCR and microarray analysis of selected clock and cell cycle-related genes in proliferating primary *Cry1^{-/-}|Cry2^{-/-}* MEF lines (n = 3 for qPCR, n = 4 for microarrays), as compared to (non-clock synchronized) proliferating WT MEF lines (n = 4 for both techniques). Note that different cell lines were used for qRT-PCR and microarray analysis. The dashed line indicates the WT level (set to 1). *p < 0.05, **p < 0.01, ***p < 0.001; Student t-test. (B) List of top five over-represented molecular and cellular functions. Transcriptome analysis was performed on proliferating primary WT and *Cry1^{-/-}|Cry2^{-/-}* MEF (four independent cell lines per genotype). The Ingenuity Pathway Analysis tool was used on differentially expressed genes (p < 0.05) with a \pm 1.2-fold change. The p value range (Fisher exact test) indicates the significance range of the various pathways and processes belonging to that function.

DeLaunay. Mice lacking *p53*⁵⁷ were obtained from The Jackson Laboratory. As required by Dutch law, all animal experiments were evaluated and approved by “DEC Consult,” an independent Animal Ethical Committee (Dutch equivalent of the Institutional Animal Care and Use Committee).

Cell culture. Primary wild-type (WT), *Cry1^{-/-}|Cry2^{-/-}*, *Cry1^{+/-}|Cry2^{-/-}*, *Cry1^{-/-}|Cry2^{+/-}*, *Bmal1^{-/-}*, *Bmal1^{+/-}|Cry1^{-/-}|Cry2^{-/-}* and *Bmal1^{-/-}|Cry1^{-/-}|Cry2^{-/-}* embryonic fibroblasts (MEFs) were isolated from 13.5E embryos and routinely cultured in DMEM/F10 (1:1) medium, containing 10% fetal calf serum and antibiotics, in a mixed gas incubator (5% CO₂ and 3% O₂) at 37°C as described before in reference 58. Primary *p53^{-/-}* MEFs have been previously generated in our lab and were kindly provided by Dr. Jay Mitchell.

Genotoxic treatment of cultured MEFs. UV sensitivity was determined as described previously in reference 59, except that the (primary) cells were plated at a higher density. In short, after removing the medium and washing the cells with PBS, Petri dish cultures were exposed to different doses of UV (254 nm, Philips TUV lamp). Mock treated control cultures went through the same procedure, except that the UV lamp was not turned on. After 3 d, the number of proliferating cells was estimated from the amount of radioactivity incorporated during a 2 h pulse with [³H]-thymidine. Cell survival was expressed as the percentage of

radioactivity in exposed cells as compared with the radioactivity in mock-treated cells.

IR sensitivity was assayed by plating early passage cells (passage 2 to 5) in triplicate in six-well plates at a density of 1,00,000 cells. The next day, cells were either gamma-irradiated (^{137}Cs γ -radiation, doses as indicated in the text) or mock treated. Cells were counted 3 d after treatment using a Coulter Multisizer Z2 (Beckman Coulter) cell counter and plotted as the percentage of the total number of cells from the corresponding mock-treated cultures.

Oxidative stress sensitivity was determined as described for the IR treatment, except that culture dishes were transferred to a 5% CO_2 /20% O_2 incubator and mock-treated control cultures were kept in the 5% CO_2 /3% O_2 incubator.

Proliferation and cell cycle distribution assays. Proliferation assays were performed by counting cells using a Coulter Multisizer Z2 (Beckman Coulter) cell counter and seeded in duplicate or triplicate in 6-well plates at a density of 100,000 cells/well. Cells were trypsinized and counted each day for 3–4 d (as indicated in the result section). Data were fitted to an exponential growth curve to determine the slope. To quantify the relative difference between cell lines with various genotypes over multiple experiments, we measured the slope of the proliferation curve. Within each experiment, the WT slope was set to 1. Cell cycle phase distribution was determined by propidium iodide/BrdU staining after 70% ethanol fixation and subsequent cell sorting (BD FACScan or a BD FACSCalibur; BD Biosciences) as described in reference 60. For MDFs, proliferation was measured by pulse-labeling cells with [^3H]-thymidine and determining the amount of incorporated radioactivity.

Real-time bioluminescent imaging. For real-time bioluminescence monitoring of circadian core oscillator performance, primary MEFs were infected with a lentiviral reporter construct expressing firefly luciferase from the *Per2* promoter.³⁸ To synchronize cells, confluent cultures were exposed to 50% horse serum for 2 h after which the cells were kept in normal medium with 10% serum for the duration of the experiment. Bioluminescence was recorded for 7 d (75 sec measurements at 10 min intervals) using a LumiCycle 32-channel automated luminometer (Actimetrics) placed in a dry, temperature-controlled incubator at 37°C as described before in reference 38.

Quantitative RT-PCR analysis. For each cell line (cultured under the same conditions as used for the proliferation assays) total RNA was isolated in duplicate or triplicate using Trizol (Invitrogen) according to the manufacturer's instructions. Quantitative RT-PCR analysis was performed by reverse transcribing 1 μg total RNA with oligo(dT) and SuperScript reverse transcriptase (Invitrogen). Subsequently quantitative PCR amplification of cDNA was performed using SYBR green and an iCyclerIQ detection system (Bio-Rad) following the manufacturer's protocol. Primers were designed to amplify a -100–250 bp

region, spanning at least one intron. Specificity was determined by melt-curve analysis and efficiency was determined by testing the primers with mixed, serially diluted cDNA. Expression levels were normalized using *Hypoxanthine phosphoribosyltransferase 1* (*Hprt1*) mRNA levels and plotted relative to WT cells.

Transcriptome analysis. MEF lines were isolated from four WT embryos (obtained from 1 pregnancy) and four *Cry1^{-/-}|Cry2^{-/-}* embryos (from two pregnancies). Each of the eight cell lines, was grown in triplicate and used for RNA isolation. Total RNA was isolated as described for qRT-PCR analysis and quality was assessed by Agilent Bioanalyzer analysis and qRT-PCR-based determination of expression levels for selected clock genes. After confirmation of RNA quality triplicate RNA samples for each cell line were pooled and processed for microarray hybridization. Synthesis of double stranded cDNA and biotin-labeled cRNA was performed according to the instructions of the manufacturer (Affymetrix). Fragmented cRNA preparations were hybridized to full mouse-genome oligonucleotide arrays (Affymetrix 430 V2.0), which were processed as described in detail before in reference 61. Significantly differentially expressed genes ($p < 0.05$ and fold-change > 1.2 up- or downregulated) were subjected to Ingenuity Pathway Analysis (Ingenuity Systems, www.ingenuity.com) to identify enriched pathways. Significance was assessed by comparing the number of found genes from the data set in a pathway to the total number of genes in that pathway using a Fisher exact test.

Statistics. For comparison of proliferative capacity, we fitted the data to an exponential growth curve. To compare groups, we used Student t-test. To compare data obtained from multiple experiments in which the WT group is set to 1 in each experiment (as in Fig. 2B), we used column statistics. All statistics were performed in GraphPad Prism 5.

Disclosure of Potential Conflicts of interest

No potential conflicts of interest were disclosed.

Acknowledgments

We would like to thank Profs. Chris Bradfield and Frank Delaunay for providing us with *Bmal1* mice. Dr. Jay Mitchell for providing us with *p53*-deficient MEFs, advice and discussions, Drs. George Garinis (ErasmusMC) and Alex Pines (LUMC) for their help with microarray data analysis. This work was supported by grants from the Netherlands Organization for Scientific Research (ZonMW Vici grant #918.36.619; ZonMW/ErasmusBio+ grant #90.201.127) and the Netherlands Genomics Initiative/Netherlands Toxicogenomics Center (grant #050-060-510) to GTJvdH.

Note

Supplemental material can be found at: www.landesbioscience.com/journals/cc/article/17974

References

- Reppert SM, Weaver DR. Coordination of circadian timing in mammals. *Nature* 2002; 418:935-41; PMID:12198538; DOI:10.1038/nature00965.
- Tyson J, Novak B. Temporal Organization of the Cell Cycle. *Curr Biol* 2008; 18:759-68; PMID:18786381; DOI:10.1016/j.cub.2008.07.001.
- Stratmann M, Schibler U. Properties, Entrainment and Physiological Functions of Mammalian Peripheral Oscillators. *J Biol Rhythms* 2006; 21:494-506; PMID:17107939; DOI:10.1177/0748730406293889.
- Balsalobre A, Damiola F, Schibler U. A Serum Shock Induces Circadian Gene Expression in Mammalian Tissue Culture Cells. *Cell* 1998; 93:929-37; PMID:9635423; DOI:10.1016/S0092-8674(00)81199-X.
- Balsalobre A, Marcacci L, Schibler U. Multiple signaling pathways elicit circadian gene expression in cultured Rat-1 fibroblasts. *Curr Biol* 2000; 10:1291-4; PMID:11069111; DOI:10.1016/S0960-9822(00)00758-2.
- Takahashi JS, Hong HK, Ko CH, McDearmon EL. The genetics of mammalian circadian order and disorder: implications for physiology and disease. *Nat Rev Genet* 2008; 9:764-75; PMID:18802415; DOI:10.1038/nrg2430.
- Kang TH, Sancar A. Circadian regulation of DNA excision repair: Implications for chrono-chemotherapy. *Cell Cycle* 2009; 8:1665-7; PMID:19411851; DOI:10.4161/cc.8.11.8707.
- Fu L, Lee CC. The circadian clock: pacemaker and tumour suppressor. *Nat Rev Cancer* 2003; 3:350-61; PMID:12724733; DOI:10.1038/nrc1072.
- Froy O. Metabolism and Circadian Rhythms. Implications for Obesity. *Endocr Rev* 2010; 31:1-24; PMID:19854863; DOI:10.1210/er.2009-0014.
- Rudic RD. Time Is of the Essence: Vascular Implications of the Circadian Clock. *Circulation* 2009; 120:1714-21; PMID:19858424; DOI:10.1161/CIRCULATIONAHA.109.853002.
- McClung CA. Circadian genes, rhythms and the biology of mood disorders. *Pharmacol Ther* 2007; 114:222-32; PMID:17395264; DOI:10.1016/j.pharmthera.2007.02.003.
- Kume K, et al. mCRY1 and mCRY2 Are Essential Components of the Negative Limb of the Circadian Clock Feedback Loop. *Cell* 1999; 98:193-205; PMID:10428031; DOI:10.1016/S0092-8674(00)81014-4.
- Griffin E, Staknis D, Weitz CJ. Light-Independent Role of CRY1 and CRY2 in the Mammalian Circadian Clock. *Science* 1999; 286:768-71; PMID:10531061; DOI:10.1126/science.286.5440.768.
- Sato TK, Yamada RG, Ukai H, Baggs JE, Miraglia LJ, Kobayashi TJ, et al. Feedback repression is required for mammalian circadian clock function. *Nat Genet* 2006; 38:312-9; PMID:16474406; DOI:10.1038/ng1745.
- Preitner N, Damiola F, Molina LL, Zakany J, Duboule D, Albrecht U, et al. The Orphan Nuclear Receptor REV-ERB α Controls Circadian Transcription within the Positive Limb of the Mammalian Circadian Oscillator. *Cell* 2002; 110:251-60; PMID:12150932; DOI:10.1016/S0092-8674(02)00825-5.
- Mukherji S, van Oudenaarden A. Synthetic biology: understanding biological design from synthetic circuits. *Nat Rev Genet* 2009; 10:859-71; PMID:19898500.
- Storch KF, Paz C, Signorovitch J, Raviola E, Pawlyk B, Li T, et al. Intrinsic Circadian Clock of the Mammalian Retina: Importance for Retinal Processing of Visual Information. *Cell* 2007; 130:730-41; PMID:17719549; DOI:10.1016/j.cell.2007.06.045.
- Lamia KA, Storch KF, Weitz CJ. Physiological significance of a peripheral tissue circadian clock. *Proc Natl Acad Sci USA* 2008; 105:15172-7; PMID:18779586; DOI:10.1073/pnas.0806717105.
- Panda S, Antoch MP, Miller BH, Su AI, Schook AB, Straume M, et al. Coordinated Transcription of Key Pathways in the Mouse by the Circadian Clock. *Cell* 2002; 109:307-20; PMID:12015981; DOI:10.1016/S0092-8674(02)00722-5.
- Storch KF, Lipan O, Leykin I, Viswanathan N, Davis FC, Wong WH, et al. Extensive and divergent circadian gene expression in liver and heart. *Nature* 2002; 417:78-83; PMID:11967526; DOI:10.1038/nature744.
- Ueda HR, Chen W, Adachi A, Wakamatsu H, Hayashi S, Takasugi T, et al. A transcription factor response element for gene expression during circadian night. *Nature* 2002; 418:534-9; PMID:12152080; DOI:10.1038/nature00906.
- Hughes ME, DiTacchio L, Hayes KR, Vollmers C, Pulivarthy S, Baggs JE, et al. Harmonics of Circadian Gene Transcription in Mammals. *PLoS Genet* 2009; 5:1000442; PMID:19343201; DOI:10.1371/journal.pgen.1000442.
- Pittendrigh CS. Temporal organization: reflections of a Darwinian clock-watcher. *Annu Rev Physiol* 1993; 55:16-54; PMID:8466172; DOI:10.1146/annurev.ph.55.030193.000313.
- Bjarnason GA, Jordan RCK, Wood PA, Qi L, Lincoln DW, Sothorn RB, et al. Circadian Expression of Clock Genes in Human Oral Mucosa and Skin: Association with Specific Cell-Cycle Phases. *Am J Pathol* 2001; 158:1793-801; PMID:11337377; DOI:10.1016/S0002-9440(01)64135-1.
- Filipski E, King VM, Etienne MC, Li X, Claustrat B, Granda TG, et al. Persistent twenty-four hour changes in liver and bone marrow despite suprachiasmatic nuclei ablation in mice. *Am J Physiol Regul Integr Comp Physiol* 2004; 287:844-51; PMID:15217787; DOI:10.1152/ajpregu.00085.2004.
- Smaaland R. Circadian rhythm of cell division. *Prog Cell Cycle Res* 1996; 2:241-66; PMID:9552400; DOI:10.1007/978-1-4615-5873-6_23.
- Nagoshi E, Saini C, Bauer C, Laroche T, Naef F, Schibler U. Circadian Gene Expression in Individual Fibroblasts: Cell-Autonomous and Self-Sustained Oscillators Pass Time to Daughter Cells. *Cell* 2004; 119:693-705; PMID:15550250; DOI:10.1016/j.cell.2004.11.015.
- Yeom M, Pendergast JS, Ohmiya Y, Yamazaki S. Circadian-independent cell mitosis in immortalized fibroblasts. *Proc Natl Acad Sci USA* 2010; 107:9665-70; PMID:20457900; DOI:10.1073/pnas.0914078107.
- Fu L, Pelicano H, Liu J, Huang P, Lee CC. The Circadian Gene Period2 Plays an Important Role in Tumor Suppression and DNA Damage Response In Vivo. *Cell* 2002; 111:41-50; PMID:12372299; DOI:10.1016/S0092-8674(02)00961-3.
- Matsuo T, Yamaguchi S, Mitsui S, Emi A, Shimoda E, Okamura H. Control Mechanism of the Circadian Clock for Timing of Cell Division in Vivo. *Science* 2003; 302:255-9; PMID:12934012; DOI:10.1126/science.1086271.
- Fu L, Patel MS, Bradley A, Wagner EF, Karsenty G. The Molecular Clock Mediates Leptin-Regulated Bone Formation. *Cell* 2005; 122:803-15; PMID:16143109; DOI:10.1016/j.cell.2005.06.028.
- Gorbacheva VY, Kondratov RV, Zhang R, Cherukuri S, Gudkov AV, Takahashi JS, et al. Circadian sensitivity to the chemotherapeutic agent cyclophosphamide depends on the functional status of the CLOCK/BMAL1 transactivation complex. *Proc Natl Acad Sci USA* 2005; 102:3407-12; PMID:15689397; DOI:10.1073/pnas.0409897102.
- Miller BH, McDearmon EL, Panda S, Hayes KR, Zhang J, Andrews JL, et al. Circadian and CLOCK-controlled regulation of the mouse transcriptome and cell proliferation. *Proc Natl Acad Sci USA* 2007; 104:3342-7; PMID:17360649; DOI:10.1073/pnas.0611724104.
- Gréchez-Cassiau A, Rayet B, Guillaumond F, Teboul M, Delaunay F. The Circadian Clock Component BMAL1 Is a Critical Regulator of p21^{WAF1/CIP1} Expression and Hepatocyte Proliferation. *J Biol Chem* 2008; 283:4535-42; PMID:18086663; DOI:10.1074/jbc.M705576200.
- Ozturk N, Lee JH, Gaddameedhi S, Sancar A. Loss of cryptochrome reduces cancer risk in p53 mutant mice. *Proc Natl Acad Sci USA* 2009; 106:2841-6; PMID:19188586; DOI:10.1073/pnas.0813028106.
- Chen-Goodspeed M, Lee CC. Tumor Suppression and Circadian Function. *J Biol Rhythms* 2007; 22:291-8; PMID:17660446; DOI:10.1177/0748730407303387.
- Pregueiro AM, Liu Q, Baker CL, Dunlap JC, Loros JJ. The Neurospora Checkpoint Kinase 2: A Regulatory Link Between the Circadian and Cell Cycles. *Science* 2006; 313:644-9; PMID:16809488; DOI:10.1126/science.1121716.
- Oklejewicz M, Destici E, Tamanini F, Hut RA, Janssens R, Van der Horst GTJ. Phase Resetting of the Mammalian Circadian Clock by DNA Damage. *Curr Biol* 2008; 18:286-91; PMID:18291650; DOI:10.1016/j.cub.2008.01.047.
- Gamsby JJ, Loros JJ, Dunlap JC. A Phylogenetically Conserved DNA Damage Response Resets the Circadian Clock. *J Biol Rhythms* 2009; 24:193-202; PMID:19465696; DOI:10.1177/0748730409334748.
- Méndez-Ferrer S, Lucas D, Battista M, Frenette PS. Haematopoietic stem cell release is regulated by circadian oscillations. *Nature* 2008; 452:442-7; PMID:18256599; DOI:10.1038/nature06685.
- van der Horst GTJ, Muijtjens M, Kobayashi K, Takano R, Kanno Si, Takao M, et al. Mammalian Cry1 and Cry2 are essential for maintenance of circadian rhythms. *Nature* 1999; 398:627-30; PMID:10217146; DOI:10.1038/19323.
- Parrinello S, Samper E, Krtolica A, Goldstein J, Melov S, Campisi J. Oxygen sensitivity severely limits the replicative lifespan of murine fibroblasts. *Nat Cell Biol* 2003; 5:741-7; PMID:12855956; DOI:10.1038/ncb1024.
- Xu Y, Yang EM, Brugarolas J, Jacks T, Baltimore D. Involvement of p53 and p21 in Cellular Defects and Tumorigenesis in Atm^{-/-} Mice. *Mol Cell Biol* 1998; 18:4385-90; PMID:9632822.
- Lowe SW, Ruley HE, Jacks T, Housman DE. p53-dependent apoptosis modulates the cytotoxicity of anticancer agents. *Cell* 1993; 74:957-67; PMID:8402885; DOI:10.1016/0092-8674(93)90719-7.
- Brown SA, Fleury-Olela F, Nagoshi E, Hauser C, Juge C, Meier CA, et al. The Period Length of Fibroblast Circadian Gene Expression Varies Widely among Human Individuals. *PLoS Biol* 2005; 3:338; PMID:16167846; DOI:10.1371/journal.pbio.0030338.
- Liu AC, Welsh DK, Ko CH, Tran HG, Zhang EE, Priest AA, et al. Intercellular Coupling Confers Robustness against Mutations in the SCN Circadian Clock Network. *Cell* 2007; 129:605-16; PMID:17482552; DOI:10.1016/j.cell.2007.02.047.
- Bunger MK, Wilsbacher LD, Moran SM, Clendenen C, Radcliffe LA, Hogenesch JB, et al. Mop3 Is an Essential Component of the Master Circadian Pacemaker in Mammals. *Cell* 2000; 103:1009-17; PMID:11163178; DOI:10.1016/S0092-8674(00)00205-1.
- Okamura H, Miyake S, Sumi Y, Yamaguchi S, Yasui A, Muijtjens M, et al. Photic Induction of mPer1 and mPer2 in Cry-Deficient Mice Lacking a Biological Clock. *Science* 1999; 286:2531-4; PMID:10617474; DOI:10.1126/science.286.5449.2531.
- Shearman LP, Stram S, Weaver DR, Maywood ES, Chaves I, Zheng B, et al. Interacting Molecular Loops in the Mammalian Circadian Clock. *Science* 2000; 288:1013-9; PMID:10807566; DOI:10.1126/science.288.5468.1013.

50. Baggs JE, Price TS, DiTacchio L, Panda S, Fitzgerald GA, Hogenesch JB. Network Features of the Mammalian Circadian Clock. *PLoS Biol* 2009; 7:52; PMID:19278294; DOI:10.1371/journal.pbio.1000052.
51. Gauger MA, Sancar A. Cryptochrome, Circadian Cycle, Cell Cycle Checkpoints and Cancer. *Cancer Res* 2005; 65:6828-34; PMID:16061665; DOI:10.1158/0008-5472.CAN-05-1119.
52. Lee S, Donehower LA, Herron AJ, Moore DD, Fu L. Disrupting Circadian Homeostasis of Sympathetic Signaling Promotes Tumor Development in Mice. *PLoS ONE* 2010; 5:10995; PMID:20539819; DOI:10.1371/journal.pone.0010995.
53. Kuilman T, Peeper DS. Senescence-messaging secretome: SMS-ing cellular stress. *Nat Rev Cancer* 2009; 9:81-94; PMID:19132009; DOI:10.1038/nrc2560.
54. Mullenders J, Fabius AZM, Madiredjo M, Bernards R, Beijersbergen RL. A Large Scale shRNA Barcode Screen Identifies the Circadian Clock Component ARNTL as Putative Regulator of the p53 Tumor Suppressor Pathway. *PLoS ONE* 2009; 4:4798; PMID:19277210; DOI:10.1371/journal.pone.0004798.
55. Michalopoulos GK, DeFrances MC. Liver Regeneration. *Science* 1997; 276:60-6; PMID:9082986; DOI:10.1126/science.276.5309.60.
56. Haus E, Smolensky MH. Biologic rhythms in the immune system. *Chronobiol Int* 1999; 16:581-622; PMID:10513884; DOI:10.3109/07420529908998730.
57. Donehower LA, Harvey M, Slagle BL, McArthur MJ, Montgomery CA, Butel JS, et al. Mice deficient for p53 are developmentally normal but susceptible to spontaneous tumours. *Nature* 1992; 356:215-21; PMID:1552940; DOI:10.1038/356215a0.
58. van de Ven M, Andresoo JO, Holcomb VB, Von Lindern M, Jong WMC, De Zeeuw CI, et al. Adaptive Stress Response in Segmental Progeria Resembles Long-Lived Dwarfism and Calorie Restriction in Mice. *PLoS Genet* 2006; 2:192; PMID:17173483; DOI:10.1371/journal.pgen.0020192.
59. Sijbers AM, De Laat WL, Ariza RR, Biggerstaf M, Wei YF, Moggs JG, et al. Xeroderma Pigmentosum Group F Caused by a Defect in a Structure-Specific DNA Repair Endonuclease. *Cell* 1996; 86:811-22; PMID:8797827; DOI:10.1016/S0092-8674(00)80155-5.
60. Smits VAJ, Van Peer MA, Essers MA, Klompmaker R, Rijksen G, Medema RH. Negative Growth Regulation of SK-N-MC Cells by bFGF Defines a Growth Factor-sensitive Point in G₂. *J Biol Chem* 2000; 275:19375-81; PMID:10770932; DOI:10.1074/jbc.M001764200.
61. Niedernhofer LJ, Garinis GA, Raams A, Lalai S, Robinson AR, Appeldoorn E, et al. A new progeroid syndrome reveals that genotoxic stress suppresses the somatotroph axis. *Nature* 2006; 444:1038-43; PMID:17183314; DOI:10.1038/nature05456.

©2011 Landes Bioscience.
Do not distribute.